11560 J. Phys. Chem. A 2005, 109, 11560−11567

MX_3^- Superhalogens (M = Be, Mg, Ca; X = Cl, Br): A Photoelectron Spectroscopic and ab Initio Theoretical Study[†]

Ben M. Elliott,[‡] Eldon Koyle,[‡] Alexander I. Boldyrev,*,[‡] Xue-Bin Wang,[§] and Lai-Sheng Wang*,[§]

Department of Chemistry and Biochemistry, 0300 Old Main Hill, Utah State University,
Logan, Utah 84322-0300, Department of Physics, 2710 University Drive, Washington State University,
Richland, Washington 99354, and W. R. Wiley Environmental Molecular Sciences Laboratory and
Chemical Sciences Division, Pacific Northwest National Laboratory, MS K8-88, P.O. Box 999,
Richland, Washington 99352

Received: July 21, 2005; In Final Form: October 5, 2005

Gas-phase alkaline earth halide anions, MgX_3^- and CaX_3^- (X = Cl, Br), were produced using electrospray and investigated using photoelectron spectroscopy at 157 nm. Extremely high electron binding energies were observed for all species and their first vertical detachment energies were measured as 6.60 ± 0.04 eV for $MgCl_3^-$, 6.00 ± 0.04 eV for $MgBr_3^-$, 6.62 ± 0.04 eV for $CaCl_3^-$, and 6.10 ± 0.04 eV for $CaBr_3^-$. The high electron binding energies indicate these are very stable anions and they belong to a class of anions, called superhalogens. Theoretical calculations at several levels of theory were carried out on these species, as well as the analogous BeX_3^-. Vertical detachment energy spectra were predicted to compare with the experimental observations, and good agreement was obtained for all species. The first adiabatic detachment energies were found to be substantially lower (by about 1 eV) than the corresponding vertical detachment energies for all the MX_3^- species, indicating extremely large geometry changes between MX_3^- and MX_3. We found that all the MX_3^- anions possess D_{3h} ($^1A_1'$) structures and are extremely stable against dissociation into MX_2 and X^-. The corresponding neutral species MX_3, however, were found to be only weakly bound with respect to dissociation toward $MX_2 + X$. The global minimum structures of all the MX_3 neutrals were found to be C_{2v} ($^2B_2$), which can be described as $(X_2^-)(MX^+)$ charge-transfer complexes, whereas the $MX_2 \cdots X$ (C_{2v}, $^2B_1$) van der Waals complexes were shown to be low-lying isomers.

Introduction

Among all the chemical elements, the halogens are known to have the highest electron affinity (EA) (3.0−3.6 eV).[1] However, molecular species are capable of exceeding the 3.617 eV (Cl)[1] atomic EA limit due to collective effects. Such species, although known and of interest since the early 1960s, were first given the moniker “superhalogens” in 1981, when a simple formula for a class of high EA species MX_{k+1} (M is a main group or transition metal atom, X is a halogen atom or a monovalent group with high EA such as CN, and k is the maximum formal valence of M) was proposed.[2] The high electron binding energy in the corresponding negative ions MX_{k+1}^- when compared to those for X^- is due to delocalization of the additional electron over k+1 X groups, as opposed to a single X. The EAs of many superhalogens have been estimated both theoretically[3−34] and experimentally.[35−58] However, direct measurements of the high electron binding energies in the MX_{k+1}^- superhalogens were not possible until recently.

In 1999, the smallest superhalogens, MX_{k+1}^- (M = Li, Na; X = Cl, Br, I), k = 1, were first studied by photoelectron spectroscopy (PES), which straightforwardly revealed the high electron binding energies of these speceis.[59] Ab initio calculations were performed and excellent agreement was found between the theoretical results and experimental data. The first vertical detachment energies (VDE’s) were measured to be 5.92 ± 0.04 ($LiCl_2^-$), 5.86 ± 0.06 ($NaCl_2^-$), 5.42 ± 0.03 ($LiBr_2^-$), 5.36 ± 0.06 ($NaBr_2^-$), 4.88 ± 0.03 (LiI_2^-), and 4.84 ± 0.06 (NaI_2^-), which are all well above the 3.617 eV electron detachment energy of Cl^-. Later studies by other groups made similar collaborative efforts on species with high EA.[60−63]

Recently, a joint theoretical and experimental study was performed for a set of higher alkali halide superhalogen systems $Na_xCl_{x+1}^-$ (x = 1−4).[64] The VDE’s were observed to increase rapidly with x to 7.0 eV for x = 4. The most stable structures for these anions were identified using a newly developed ab initio gradient embedded genetic algorithm. The good agreement between theory and experiment confirmed the structure of these species.

Superhalogens involving alkaline earth atoms (MX_3^-) have been studied by several groups.[18,25,65,66] Most recently, Skurski and co-workers performed extensive studies on several alkali earth halide superhalogen species, MX_3^- (M = Be, Mg, Ca; X = F, Cl, Br), as well as species with mixed halide ligands.[65,66] Extremely high VDE’s were reported for these species and several of these are beyond the 157 nm (7.866 eV) photon energy (the highest photodetachment laser energy available in our lab): BeF_3^- (8.472 eV), MgF_3^- (8.793 eV), CaF_3^- (8.620 eV), all with F^- ligands. In general, species with Cl^- or Br^- ligands have lower VDE’s.

[†] Part of the special issue “Jack Simons Festschrift”.

* Corresponding authors. E-mail: A.I.B., boldyrev@cc.usu.edu; L.-S.W., ls.wang@pnl.gov.

[‡] Utah State University.

[§] Washington State University.

10.1021/jp054036v CCC: $30.25

In the present contribution, we report a joint experimental and theoretical investigation on four alkali earth halide superhalogens, MX_3^- (M = Mg, Ca; X = Cl, Br) using PES and ab initio calculations. Well resolved spectral features were observed and interpreted using the theoretical results. The corresponding neutral species were also investigated theoretically, allowing their structures and stabilities to be elucidated.

Experimental Method

The experiment was carried out with a PES apparatus equipped with a magnetic-bottle time-of-flight photoelectron analyzer and an electrospray ionization source. Details of the experimental method have been given elsewhere.[67] Briefly, the anions of interest, MX_3^- (M = Mg, Ca; X = Cl, Br), were produced from electrospray of 10^{-3} M solutions of the corresponding MX_2 salts in H_2O/CH_3OH (1/3 volume ratio) mixed solvent. Anions produced from the electrospray source were guided into a quadruple ion trap, where ions were accumulated for 0.1 s before being pulsed into the extraction zone of a time-of-flight mass spectrometer.

During the PES experiment, each MX_3^- species was mass-selected and decelerated before being intercepted by a probe laser beam in the photodetachment zone of the magnetic-bottle photoelectron analyzer. In the current study, photoelectron spectra were only obtained at 157 nm (7.866 eV) from an F_2 excimer laser due to the expected high electron detachment energies of these species. All experiments were performed at 20 Hz repetition rate with the ion beam off at alternating laser shots for background subtraction, which was critical for high photon energy experiments (>4.661 eV) due to background noises. Photoelectrons were collected at nearly 100% efficiency by the magnetic-bottle and analyzed in a 4-meter long electron flight tube. Photoelectron time-of-flight spectra were collected and then converted to kinetic energy spectra, calibrated by the known spectra of I^- and O^-. The electron binding energy spectra presented were obtained by subtracting the kinetic energy spectra from the detachment photon energies. The electron kinetic energy resolution ($\Delta E/E$) was about 2%, i.e., ~10 meV for 0.5 eV electrons, as measured from the spectrum of I^- at 355 nm.

Theoretical Methods

The structures of all four MX_3^- superhalogens and their corresponding neutrals were first optimized, and harmonic frequencies were obtained using the hybrid density functional (DFT) method, B3LYP,[68−71] and the polarized split-valence basis sets, 6-311+G*.[72−77] The B3LYP structures were then refined at the MP2[78−80] and CCSD(T)[81−88] levels using the same basis sets. Single point calculations were run at the CCSD(T) level with the more extended 6-311+G(2df) basis.

The VDE's were then calculated for comparison with the experimental PES data. We used the restricted outer valence Green Function method (ROVGF)[89−93] as our main tool for computing the VDE's. Further calculations were done using the time-dependent DFT (TD-B3LYP)[94−96] and the ΔCCSD(T) (energy differences between a given anion and the various states of its corresponding neutral) methods. At the TD-B3LYP level of theory the vertical electron detachment energies were calculated as a sum of the lowest transitions from the singlet anion into the final lowest doublet state of the neutral species (at the B3LYP level of theory) and the vertical excitation energies in the neutral species (at the TD-B3LYP level of theory). The 6-311+G(2df) basis sets were used for all VDE calculations.

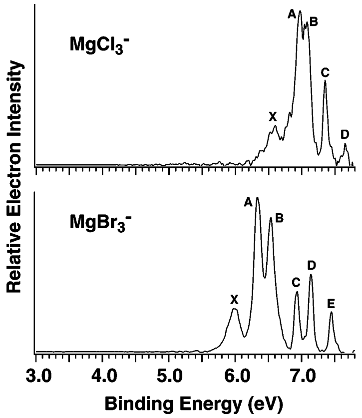

Figure 1. Photoelectron spectra of $MgCl_3^-$ and $MgBr_3^-$ at 157 nm (7.866 eV).

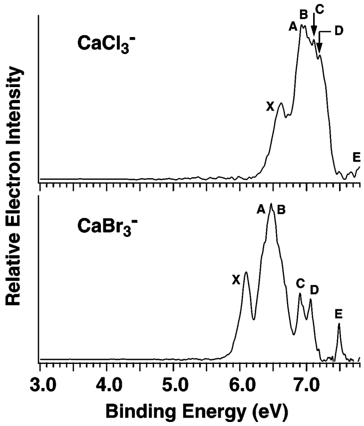

Figure 2. Photoelectron spectra of $CaCl_3^-$ and $CaBr_3^-$ at 157 nm (7.866 eV).

TABLE 1: Experimental Vertical Detachment Energies (eV) for the MX_3^- Anions (M = Mg, Ca; X = Cl, Br) from the Photoelectron Spectra in Figures 1 and 2 (Uncertainty = 0.04 eV)

	X	A	B	C	D	E
$MgCl_3^-$	6.60	6.97	7.08	7.35	7.65	
$MgBr_3^-$	6.00	6.34	6.54	6.93	7.14	7.45
$CaCl_3^-$	6.62	6.95	~7.0	7.11	7.20	~7.8
$CaBr_3^-$	6.10	~6.4	~6.5	6.90	7.06	7.49

Finally, a check was done on the performance of DFT methods for these systems. Geometry optimizations and the PES were calculated using the BPW91[97−102] and TD-BPW91 methods on the main species of interest, MX_3^-, with the 6-311+G* and 6-311+G(2df) basis sets, respectively. All calculations were performed using the Gaussian 03[103] quantum chemical calculation package, except for the ROVGF which were run with Gaussian 98.[104]

Experimental Results

Figures 1 and 2 show the 157 nm spectra of MgX_3^- and CaX_3^- (X = Cl, Br), respectively. All species investigated here exhibit extremely high electron detachment energies, as expected. Five well resolved bands are observed for $MgCl_3^-$ and their VDE's are given in Table 1. The first band with a VDE of 6.60 ± 0.04 eV is relatively weak and very broad, suggesting a large geometry change between the ground states of $MgCl_3^-$ and $MgCl_3$. The detachment threshold of the ground-state band is about 6.3 eV, which may not represent the ADE because the 0−0 transition may have a negligible Franck−Condon factor. Bands A and B, which are the most intense peaks, are partially

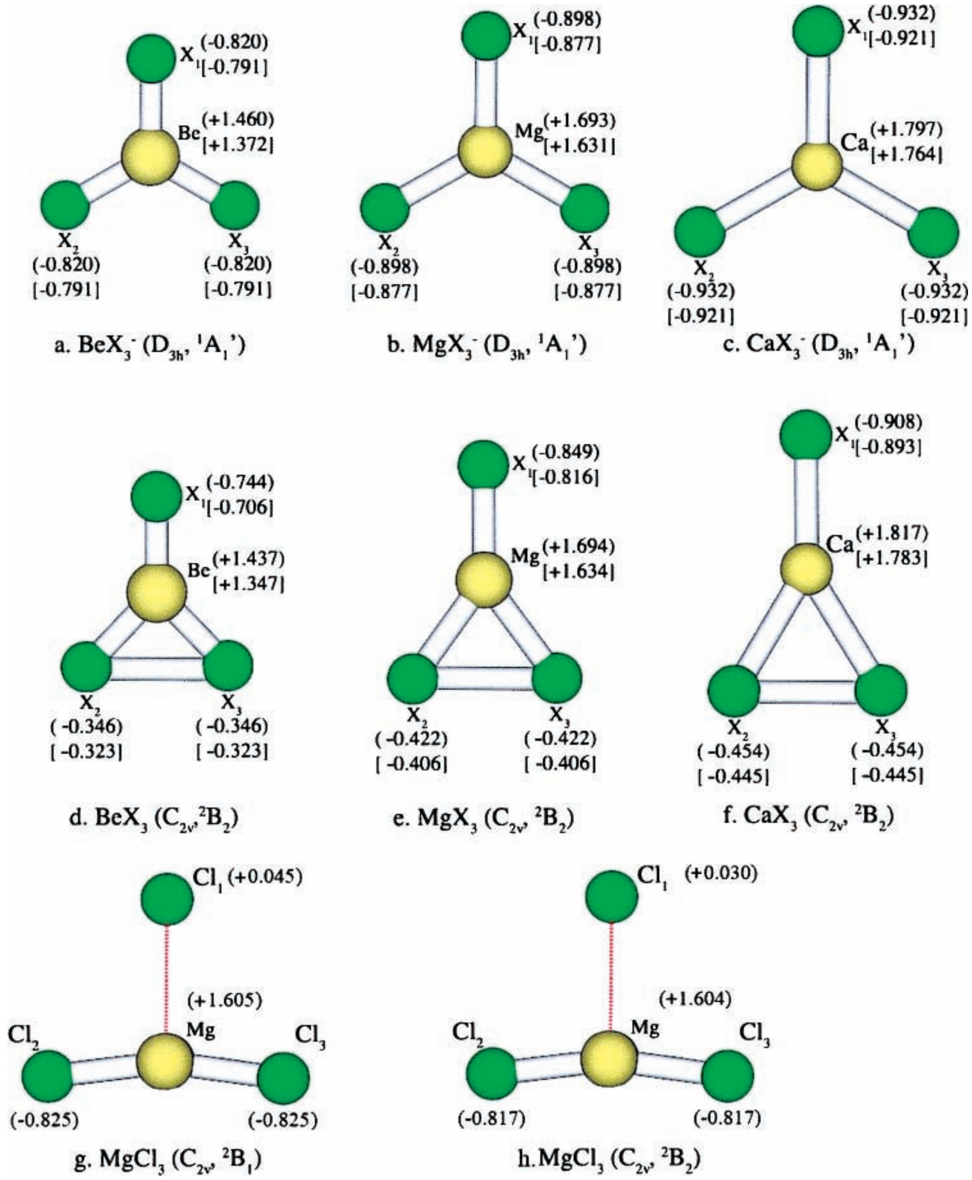

Figure 3. Molecular structures of the MX_3^- and MX_3 species studied. See tables for relevant molecular properties. Values in parentheses and brackets give atomic charges (NBO) when X is Cl and Br, respectively, at the MP2/6-311+G* level of theory.

overlapping. Bands C and D are well separated and appear to be very sharp. $MgBr_3^-$ has lower electron binding energies than $MgCl_3^-$ and the VDE of its ground-state transition is 6.00 ± 0.04 eV. The spectral features of $MgBr_3^-$ are similar to those of $MgCl_3^-$ but are much well resolved; in particular, bands A and B are better separated. An extra band (E) was also observed in the spectrum of $MgBr_3^-$. The VDE's for all the observed bands for $MgBr_3^-$ are also given in Table 1.

The photoelectron spectra of the two CaX_3^- anions (Figure 2) are more congested compared to the those for the corresponding MgX_3^- species. For $CaCl_3^-$, only the ground-state band (X) was well resolved with a VDE of 6.62 ± 0.04 eV, which is slightly higher than that of $MgCl_3^-$. $CaBr_3^-$ also has lower binding energies than $CaCl_3^-$ and its first VDE is measured to be 6.10 ± 0.04 eV. The spectrum of $CaBr_3^-$ is better separated and is very similar to that of $MgBr_3^-$, except that bands A and B overlap in the spectrum of $CaBr_3^-$. In comparison to the spectrum of $CaBr_3^-$, we note that the bands A, B, C, and D in the spectrum of $CaCl_3^-$ all overlap with each other, giving the broad features between 6.8 and 7.4 eV. There also seemed to exist a very weak band (E) at binding energy ~7.5 eV, which appeared to be cut off in the spectrum of $CaCl_3^-$. The estimated VDE's for the features for $CaCl_3^-$ and $CaBr_3^-$ are also given in Table 1. The X band in both spectra of CaX_3^- (Figure 2) are also relatively broad, similar to that of the MgX_3^- species, again indicating substantial geometric changes upon removal of the extra electron.

Theoretical Results

In our theoretical calculations, we also included the BeX_3^- species for completeness. We found the six MX_3^- (M = Be, Mg, Ca; X = Cl, Br) all have perfectly planar (D_{3h}, $^1A_1'$) structures (Figure 3, structures a−c) with the same valence electronic configuration ($1a_1'^2 1e'^4 2a_1'^2 2e'^4 3e'^4 1a_2''^2 1e''^4 1a_2'^2$). As can be seen (Table 2), the only independent geometrical parameter R(M−X) agrees well at all levels of theory employed for all the MX_3^- anions, and our results agree well with those previously published.[65,66]

For the neutral MX_3 species we found the lowest geometry structures correspond to the C_{2v} ($^2B_2$) structure (Figure 3d−f, Table 3). This structure can be formally described as a

TABLE 2: Molecular Properties of the MX_3^- Species

	$BeCl_3^-$ (D_{3h}, $^1A_1'$)			$BeBr_3^-$ (D_{3h}, $^1A_1'$)		
molecular parameter	B3LYP/ 6-311+G*	MP2/ 6-311+G*	CCSD(T)/ 6-311+G* [b]	B3LYP/ 6-311+G*	MP2/ 6-311+G*	CCSD(T)/ 6-311+G* [c]
E, au	−1395.75229	−1393.93547	−1393.98409	−7737.50680	−7732.47292	−7732.51564
R(Be−X), Å	1.939	1.922	1.926	2.104	2.092	2.098
ω_1 (e′), cm^{-1}	718 (358.0)[a]	770 (362.7)[a]	763	617 (311.1)[a]	666 (316.7)[a]	659
ω_2 (e′), cm^{-1}	172 (1.2)[a]	176 (1.6)[a]	175	104 (0.1)[a]	108 (0.2)[a]	107
ω_3 (a$_2''$), cm^{-1}	355 (31.2)[a]	366 (30.7)[a]	365	307 (11.6)[a]	312 (12.5)[a]	313
ω_4 (a$_1'$), cm^{-1}	327 (0.0)[a]	342 (0.0)[a]	340	196 (0.0)[a]	206 (0.0)[a]	204

	$MgCl_3^-$ (D_{3h}, $^1A_1'$)			$MgBr_3^-$ (D_{3h}, $^1A_1'$)		
molecular parameter	B3LYP/ 6-311+G*	MP2/ 6-311+G*	CCSD(T)/ 6-311+G* [d]	B3LYP/ 6-311+G*	MP2/ 6-311+G*	CCSD(T)/ 6-311+G* [e]
E, au	−1581.11427	−1578.90610	−1578.95346	−7922.88249	−7917.46052	−7919.50210
R(Mg−X), Å	2.293	2.275	2.280	2.450	2.439	2.442
ω_1 (e′), cm^{-1}	437 (159.8)[a]	462 (161.3)[a]	460	367 (131.4)[a]	383 (134.2)[a]	381
ω_2 (e′), cm^{-1}	104 (1.8)[a]	106 (9.0)[a]	106	67 (2.0)[a]	67 (2.4)[a]	67
ω_3 (a$_1'$), cm^{-1}	266 (0.0)[a]	280 (0.0)[a]	279	164 (0.0)[a]	171 (0.0)[a]	170
ω_4 (a$_2''$), cm^{-1}	167 (50.3)[a]	176 (53.9)[a]	176	143 (26.1)[a]	144 (29.5)[a]	144

	$CaCl_3^-$ (D_{3h}, $^1A_1'$)			$CaBr_3^-$ (D_{3h}, $^1A_1'$)		
molecular parameter	B3LYP/ 6-311+G*	MP2/ 6-311+G*	CCSD(T)/ 6-311+G* [f]	B3LYP/ 6-311+G*	MP2/ 6-311+G*	CCSD(T)/ 6-311+G* [g]
E, au	−2058.64642	−2056.23659	−2056.30100	−8400.41704	−8394.79970	−8394.85775
R(Ca−X), Å	2.566	2.561	2.566	2.721	2.720	2.726
ω_1 (e′), cm^{-1}	332 (152.8)[a]	346 (148.0)[a]	344	269 (108.2)[a]	284 (106.7)[a]	282
ω_2 (e′), cm^{-1}	75 (7.5)[a]	80 (9.9)[a]	80	50 (2.0)[a]	51 (2.9)[a]	51
ω_3 (a$_1'$), cm^{-1}	237 (0.0)[a]	243 (0.0)[a]	242	145 (0.0)[a]	150 (0.0)[a]	150
ω_4 (a$_2''$), cm^{-1}	92 (68.8)[a]	100 (75.7)[a]	100	81 (39.0)[a]	85 (44.3)[a]	84

[a] Values in parentheses represent relative absorbance intensities in the IR spectrum. [b] E_{tot} = −1394.1655056 au. [c] E_{tot} = −7732.63950 au. [d] E_{tot} = −1579.146627 au. [e] E_{tot} = −7917.632111 au. [f] E_{tot} = −2056.561720 au. [g] E_{tot} = −8395.056541 au (all at CCSD(T)/6-311+G(2df)//CCSD(T)/6-311+G*).

$(X_2^-)(MX^+)$ complex. We optimized geometric parameters and calculated harmonic frequencies for Cl_2^-, Br_2^-, $BeCl^+$, $MgCl^+$, $CaCl^+$, $BeBr^+$, $MgCl^+$, and $CaCl^+$ species (Tables S1 and S2, Supporting Information), which match rather well the properties in the corresponding fragments in the C_{2v} ($^2B_2$) MX_3 structures. The calculated NBO charges also support the $(X_2^-)(MX^+)$ description with the unpaired electron completely localized on the X_2^- fragment. We performed a detailed search on the van der Waals portion of the potential energy surface for $MgCl_3$ and found no other local minima at the B3LYP/6-311+G* level of theory. However, we found a less stable local minimum corresponding to a van der Waals MX_2···X complex for the neutral MX_3 species at the CCSD(T)/6-311+G* level of theory. The unpaired electron on the X atom can be oriented in plane ($^2B_2$, state), perpendicular to the plane ($^2B_1$ state), or along the C_2 molecular axis ($^2A_1$ state). At the CCSD(T)/6-311+G* level of theory the potential energy curve was completely repulsive for the $^2A_1$ state, geometry optimization for the $^2B_2$ state leads to a structure which is a first-order saddle point (Figure 3h and Table 4). Geometry optimization following the imaginary mode for the $^2B_2$, state leads to the $(X_2^-)(MX^+)$ global minimum structure. We found a weakly bound local minimum (4.29 kcal/mol (CCSD(T)/6-311+G(2df)//CCSD(T)/6-311+G*+ZPE//CCSD(T)/6-311+G*) with respect to $MgCl_2$ ($D_{\infty h}$, $^1\Sigma_g^+$) + Cl (^2P) asymptotic limit for the $^2B_1$ state (Figure 3g and Table 4). One can see that the X_2−M−X_3 angle is close to 180° and the M···X_1 distance is rather long, clearly indicating a van der Waals interaction. The small vibrational frequencies corresponding to the MX_2···X vibrational modes is consistent with the weak interaction. Because for $MgCl_3$ the MX_2···X [C_{2v} ($^2B_1$)] van der Waals local minimum was found to be appreciably higher in energy than the global minimum $(X_2^-)(MX^+)$ structure (by 14.3 kcal/mol at CCSD(T)/6-311+G(2df)/CCSD(T)/6-311+G*+ZPE//CCSD(T)/6-311+G*), we did not perform any study on van der Waals local minima for other MX_2···X complexes.

Comparison Between Calculated VDE's and the Photoelectron Spectra. *$MgCl_3^-$*. The ab initio VDE's calculated at the TD-B3LYP/6-311+G(2df), ROVGF/6-311+G(2df) and CCSD(T)/6-311+G(2df) levels for $MgCl_3^-$ are compared to the experimental values in Table 5. One can see immediately that the ROVGF and CCSD(T) values agree well not only with each other but also with the experimental data. However, the theoretical VDE's calculated at the TD-B3LYP/6-311+G(2df) level of theory are completely off. We also calculated the theoretical VDE's of $MgCl_3^-$ using the BPW91/6-311+G(2df) level of theory (Supporting Information Table S2), and the results at this level of theory are even farther from the experiment. Clearly, both DFT methods failed for this anion. The first VDE corresponding to electron detachment from the $1a_2''$-HOMO (pure ligand MO) calculated at ROVGF/6-311+G(2df) and CCSD(T)/6-311+G(2df) is 6.65 and 6.50 eV, respectively, and they are in excellent agreement with the experimental value of 6.60 eV. Our theoretical VDE for the ground-state transition for $MgCl_3^-$ is also in good agreement with the value calculated previously (6.684 eV).[66] The first ADE calculated at CCSD(T)/6-311+G(2df) level is 5.61 eV relative to the $(Cl_2^-)(MgCl^+)$ neutral global minimum. The large difference between the ADE and VDE reflects the significant geometry change upon electron detachment, consistent with the broad ground detachment band (Figure 1). Thus, experimentally, the ADE is not accessible because of the negligible Franck−Condon factor for the 0−0 transition due to the large anion to neutral geometry change. The pole strength for all the detach-

TABLE 3: Molecular Properties of the C_{2v} ($^2B_2$) Neutral MX_3 Structures

	$BeCl_3$ (C_{2v}, $^2B_2$)			$BeBr_3$ (C_{2v}, $^2B_2$)		
molecular parameter	B3LYP/6-311+G*	MP2/6-311+G*	CCSD(T)/6-311+G* [b]	B3LYP/6-311+G*	MP2/6-311+G*	CCSD(T)/6-311+G* [c]
E, au	−1395.55443	−1393.73788	−1393.79069	−7737.32483	−7732.29022	−7732.33640
R(Be−X$_1$), Å	1.827	1.815	1.820	1.987	1.979	1.985
R(Be−X$_{2,3}$), Å	1.962	1.944	1.950	2.126	2.115	2.121
∠(X$_2$−Be−X$_3$), deg	89.0	86.4	87.3	89.3	86.4	87.2
ω_1 (a$_1$), cm^{-1}	918 (330.9)[a]	1002 (432.0)[a]	986	803 (316.2)[a]	869 (399.2)[a]	855
ω_2 (a$_1$), cm^{-1}	344 (0.4)[a]	368 (0.0)[a]	362	210 (0.1)[a]	224 (0.0)[a]	220
ω_3 (a$_1$), cm^{-1}	174 (0.2)[a]	219 (1.3)[a]	212	110 (0.1)[a]	138 (0.4)[a]	133
ω_4 (b$_2$), cm^{-1}	495 (7.6)[a]	908 (653.3)[a]	514	429 (13.4)[a]	577 (796.6)[a]	437
ω_5 (b$_2$), cm^{-1}	144 (2.1)[a]	165 (15.8)[a]	158	91 (0.5)[a]	99 (2.8)[a]	97
ω_6 (b$_1$), cm^{-1}	273 (34.0)[a]	284 (32.3)[a]	286	243 (16.9)[a]	240 (17.1)[a]	242

	$MgCl_3$ (C_{2v}, $^2B_2$)			$MgBr_3$ (C_{2v}, $^2B_2$)		
molecular parameter	B3LYP/6-311+G*	MP2/6-311+G*	CCSD(T)/6-311+G* [d]	B3LYP/6-311+G*	MP2/6-311+G*	CCSD(T)/6-311+G* [e]
E, au	−1580.91156	−1578.70301	−1578.75427	−7922.69424	−7917.27162	−7917.31633
R(Mg−X$_1$), Å	2.195	2.179	2.181	2.343	2.336	2.339
R(Mg−X$_{2,3}$), Å	2.347	2.326	2.328	2.501	2.491	2.494
∠(X$_2$−Mg−X$_3$), deg	73.4	71.1	72.1	74.8	72.2	73.1
ω_1 (a$_1$), cm^{-1}	553 (167.5)[a]	591 (176.2)[a]	587	470 (150.8)[a]	479 (159.9)[a]	494
ω_2 (a$_1$), cm^{-1}	281 (0.5)[a]	303 (0.1)[a]	298	176 (0.1)[a]	189 (0.0)[a]	185
ω_3 (a$_1$), cm^{-1}	163 (3.2)[a]	192 (3.9)[a]	184	103 (1.1)[a]	125 (1.3)[a]	120
ω_4 (b$_2$), cm^{-1}	279 (4.6)[a]	447 (1218.6)[a]	286	228 (8.9)[a]	278 (151.5)[a]	224
ω_5 (b$_2$), cm^{-1}	81 (15.0)[a]	92 (40.0)[a]	85	56 (5.3)[a]	61 (10.4)[a]	58
ω_6 (b$_1$), cm^{-1}	119 (47.1)[a]	124 (49.9)[a]	124	103 (29.4)[a]	104 (32.3)[a]	104

	$CaCl_3$ (C_{2v}, $^2B_2$)			$CaBr_3$ (C_{2v}, $^2B_2$)		
molecular parameter	B3LYP/6-311+G*	MP2/6-311+G*	CCSD(T)/6-311+G* [f]	B3LYP/6-311+G*	MP2/6-311+G*	CCSD(T)/6-311+G* [g]
E, au	−2058.44524	−2056.03573	−2056.10365	−8400.22873	−8394.61144	−8394.67212
R(Ca−X$_1$), Å	2.463	2.467	2.473	2.617	2.626	2.633
R(Ca−X$_{2,3}$), Å	2.642	2.631	2.639	2.792	2.788	2.796
∠(X$_2$−Ca−X$_3$), deg	63.8	61.4	62.1	65.6	63.0	63.6
ω_1 (a$_1$), cm^{-1}	398 (199.1)[a]	416 (197.9)[a]	412	331 (154.8)[a]	347 (157.8)[a]	343
ω_2 (a$_1$), cm^{-1}	248 (1.4)[a]	266 (0.1)[a]	260	156 (0.1)[a]	171 (0.0)[a]	166
ω_3 (a$_1$), cm^{-1}	159 (3.9)[a]	187 (5.6)[a]	181	102 (0.9)[a]	123 (1.4)[a]	118
ω_4 (b$_2$), cm^{-1}	219 (4.5)[a]	298 (35.9)[a]	216	171 (9.1)[a]	191 (9.1)[a]	167
ω_5 (b$_2$), cm^{-1}	45 (27.7)[a]	50 (39.0)[a]	49	34 (12.2)[a]	36 (16.7)[a]	35
ω_6 (b$_1$), cm^{-1}	29 (56.5)[a]	38 (61.9)[a]	38	30 (38.2)[a]	34 (42.5)[a]	33

[a] Values in parentheses represent relative absorbance intensities in the IR spectrum (km/mol). [b] $E_{tot} = -1393.964155$ au. [c] $E_{tot} = -7732.45384$ au. [d] $E_{tot} = -1578.940444$ au. [e] $E_{tot} = -7917.440299$ au [f] $E_{tot} = -2056.362176$ au. [g] $E_{tot} = -8394.868974$ au (all at CCSD(T)/6-311+G(2df)//CCSD(T)/6-311+G*).

TABLE 4: Molecular Properties of the $MgCl_3$ (C_{2v}, $^2B_1$) and $MgCl_3$ (C_{2v}, $^2B_2$) van der Waals Complexes

molecular parameter	$MgCl_3$ (C_{2v}, $^2B_2$) CCSD(T)/6-311+G*	$MgCl_3$ (C_{2v}, $^2B_1$) CCSD(T)/6-311+G*
E, au	−1578.74231	−1578.73515
R(Mg−Cl$_1$), Å	2.527	2.750
R(Mg−Cl$_{2,3}$), Å	2.202	2.195
∠(Cl$_1$−Mg−Cl$_{2,3}$), deg	97.3	99.8
ω_1(b$_2$), cm^{-1}	587	612
ω_2(b$_2$), cm^{-1}	90 i	72
ω_3(a$_1$), cm^{-1}	326	334
ω_4(a$_1$), cm^{-1}	214	147
ω_5(a$_1$), cm^{-1}	95	100
ω_6(b$_1$), cm^{-1}	124	118

TABLE 5: Comparison of the Experimental VDE's to Calculated VDE's at Three Levels of Theory for $MgCl_3^-$ and $MgBr_3^-$

			VDE(theo), eV		
feature	VDE(exp), eV	molecular orbital	TD-B3LYP/6-311+G(2df)	OVGF/6-311+G(2df)	ΔCCSD(T)/6-311+G(2df)
			$MgCl_3^-$ (D_{3h}, $^1A_1'$)		
X	6.60	1a$_2'$	5.76	6.65 (0.907)[a]	6.50
A	6.97	1e$''$	6.02	6.97 (0.909)[a]	6.82
B	7.08	3e$'$	6.26	7.03 (0.908)[a]	6.87
C	7.35	1a$_2''$	6.48	7.27 (0.908)[a]	
D	7.65	2e$'$	6.94	7.73 (0.907)[a]	
		2a$_1'$	7.70	8.71 (0.909)[a]	
			$MgBr_3^-$ (D_{3h}, $^1A_1'$)		
X	6.00	1a$_2'$	5.33	6.14 (0.908)[a]	6.03
A	6.34	1e$''$	5.57	6.46 (0.910)[a]	6.36
B	6.54	3e$'$	5.82	6.50 (0.909)[a]	6.38
C	6.93	1a$_2''$	6.01	6.77 (0.911)[a]	
D	7.14	2e$'$	6.51	7.24 (0.908)[a]	
E	7.45	2a$_1'$	7.38	8.33 (0.907)[a]	

[a] Values in parentheses represent the pole strength of the OVGF calculation.

ment channels are higher than 0.9, thus justifying the use of the ROVGF calculations.

$MgBr_3^-$. The calculated VDE's for $MgBr_3^-$ (Table 5) are also in good agreement with the experimental data at ROVGF/6-311+G(2df) and CCSD(T)/6-311+G(2df) for all the observed bands except for the band E at the highest binding energy, possibly due to the failure of OVGF at such high energies. The first VDE's calculated at ROVGF/6-311+G(2df) and CCSD(T)/6-311+G(2df) are 6.14 and 6.03 eV, respectively, and these values are in excellent agreement with the experimental value 6.00 eV (Table 5). Our theoretical VDE of $MgBr_3^-$ is also in

good agreement with the value calculated previously (6.144 eV).[66] The first ADE for $MgBr_3^-$ is 5.22 eV (CCSD(T)/6-311+G(2df)), which is also significantly lower than the first VDE.

$CaCl_3^-$. The calculated VDE's for the two CaX_3^- species are compared with the experimental data in Table 6. The $CaCl_3^-$ superhalogen has a slightly higher first VDE than that of $MgCl_3^-$. The Cl···Cl distance in $CaCl_3^-$ is larger than in $MgCl_3^-$ because of the longer Ca−Cl bond length, and therefore the Coulomb repulsion between the ligands is smaller in the former, which could stabilize the HOMO and increase the first VDE. The calculations show that the VDE's for the HOMO−1 (1e″), HOMO−2 ($1a_2''$), HOMO−3 (3e′), and HOMO−4 (2e′) are very close to each other, consistent with the congested photoelectron spectrum observed for $CaCl_3^-$ (Figure 2). The first VDE at ROVGF/6-311+G(2df) (6.68 eV) and CCSD(T)/6-311+G(2df) (6.51 eV) agrees well with the experimental value (6.62 eV), but it is appreciably off (5.72 eV) at B3LYP/6-311+G(2df). Our theoretical and experimental first VDE of $CaCl_3^-$ agrees well with the value calculated previously 6.732 eV.[66] The first ADE is 5.42 eV (CCSD(T)/6-311+G(2df)), which is again considerably smaller than the VDE due to the large geometry change between the anion and neutral ground states.

$CaBr_3^-$. The calculated VDE's for $CaBr_3^-$ are also in good agreement with the experimental data at the OVGF level of theory, but off at the TD-B3LYP level (Table 6). Our theoretical VDE for the ground-state transition of $CaCl_3^-$ agrees well with the value calculated previously (6.238 eV).[66] The calculated ADE for $CaBr_3^-$ is 5.10 eV (CCSD(T)/6-311+G(2df)).

BeX_3^-. Although the photoelectron spectra of the beryllium halide species are not available experimentally, we predicted their VDE's for comparison (Table 7). The first VDE's were calculated to be 6.15 eV (ROVGF/6-311+G(2df)) and 6.01 eV (CCSD(T)/6-311+G(2df)) for $BeCl_3^-$ and 5.65 eV (ROVGF/6-311+G(2df)) and 5.55 eV (CCSD(T)/6-311+G(2df)) for $BeBr_3^-$. The calculated VDE's for the BeX_3^- species are smaller than those for the MgX_3^- species, following the trend observed between MgX_3^- and CaX_3^-. Our predicted VDE's are in good agreement with the values calculated previously, 6.171 eV (ROVGF/6-311+G(3df)) and 6.027 eV (CCSD(T)/6-311+G(3df)) for $BeCl_3^-$ and 5.647 eV (ROVGF/6-311+G(3df)) and 5.549 eV (CCSD(T)/6-311+G(3df)) for $BeBr_3^-$, by Anusiewicz and Skurski.[65] Our calculated ADE's are 5.48 eV for $BeCl_3^-$ and 5.05 for $BeBr_3^-$.

Stabilities of the Alkaline Earth Superhalogens. The anions are very strongly bound species against removal of a halide anion (eqs 1−3) or X_2 molecule (eqs 4−6) (all at CCSD(T)/6-311+G(2df)+ZPE/CCSD(T)/6-311+G*) with the first dissociation channel being substantially lower.

$$BeX_3^- (D_{3h}, {}^1A_1') \rightarrow BeX_2 (D_{\infty h}, {}^1\Sigma_g^+) + X^- ({}^1S) \qquad \Delta E(X{=}Cl) = +62.8 \text{ kcal/mol} \quad \Delta E(X{=}Br) = +54.7 \text{ kcal/mol} \tag{1}$$

$$MgX_3^- (D_{3h}, {}^1A_1') \rightarrow MgX_2 (D_{\infty h}, {}^1\Sigma_g^+) + X^- ({}^1S) \qquad \Delta E(X{=}Cl) = +70.5 \text{ kcal/mol} \quad \Delta E(X{=}Br) = +63.3 \text{ kcal/mol} \tag{2}$$

$$CaX_3^- (D_{3h}, {}^1A_1') \rightarrow CaX_2 (D_{\infty h}, {}^1\Sigma_g^+) + X^- ({}^1S) \qquad \Delta E(X{=}Cl) = +68.8 \text{ kcal/mol} \quad \Delta E(X{=}Br) = +63.9 \text{ kcal/mol} \tag{3}$$

$$BeX_3^- (D_{3h}, {}^1A_1') \rightarrow BeX^- (C_{\infty v}, {}^1\Sigma^+) + X_2 (D_{\infty h}, {}^1\Sigma_g^+) \qquad \Delta E(X{=}Cl) = +189.6 \text{ kcal/mol} \quad \Delta E(X{=}Br) = +169.4 \text{ kcal/mol} \tag{4}$$

$$MgX_3^- (D_{3h}, {}^1A_1') \rightarrow MgX^- (C_{\infty v}, {}^1\Sigma^+) + X_2 (D_{\infty h}, {}^1\Sigma_g^+) \qquad \Delta E(X{=}Cl) = +169.2 \text{ kcal/mol} \quad \Delta E(X{=}Br) = +153.3 \text{ kcal/mol} \tag{5}$$

$$CaX_3^- (D_{3h}, {}^1A_1') \rightarrow CaX^- (C_{\infty v}, {}^1\Sigma^+) + X_2 (D_{\infty h}, {}^1\Sigma_g^+) \qquad \Delta E(X{=}Cl) = +174.9 \text{ kcal/mol} \quad \Delta E(X{=}Br) = +164.2 \text{ kcal/mol} \tag{6}$$

However, the neutral MX_3 species are considerably more weakly bound. Equations 7−12 show the calculated dissociation energies for the ground-state MX_3 species at CCSD(T)/6-311+G(2df):

$$BeX_3 (C_{2v}, {}^2B_2) \rightarrow BeX_2 (D_{\infty h}, {}^1\Sigma_g^+) + X ({}^2P) \qquad \Delta E(X{=}Cl) = +14.0 \text{ kcal/mol} \quad \Delta E(X{=}Br) = +14.2 \text{ kcal/mol} \tag{7}$$

$$MgX_3 (C_{2v}, {}^2B_2) \rightarrow MgX_2 (D_{\infty h}, {}^1\Sigma_g^+) + X ({}^2P) \qquad \Delta E(X{=}Cl) = +18.7 \text{ kcal/mol} \quad \Delta E(X{=}Br) = +19.2 \text{ kcal/mol} \tag{8}$$

$$CaX_3 (C_{2v}, {}^2B_2) \rightarrow CaX_2 (D_{\infty h}, {}^1\Sigma_g^+) + X ({}^2P) \qquad \Delta E(X{=}Cl) = +21.2 \text{ kcal/mol} \quad \Delta E(X{=}Br) = +22.6 \text{ kcal/mol} \tag{9}$$

$$BeX_3 (C_{2v}, {}^2B_2) \rightarrow BeX (C_{\infty v}, {}^2\Sigma^+) + X_2 (D_{\infty h}, {}^1\Sigma_g^+) \qquad \Delta E(X{=}Cl) = +89.6 \text{ kcal/mol} \quad \Delta E(X{=}Br) = +82.7 \text{ kcal/mol} \tag{10}$$

$$MgX_3 (C_{2v}, {}^2B_2) \rightarrow MgX (C_{\infty v}, {}^2\Sigma^+) + X_2 (D_{\infty h}, {}^1\Sigma_g^+) \qquad \Delta E(X{=}Cl) = +74.8 \text{ kcal/mol} \quad \Delta E(X{=}Br) = +70.3 \text{ kcal/mol} \tag{11}$$

$$CaX_3 (C_{2v}, {}^2B_2) \rightarrow CaX (C_{\infty v}, {}^2\Sigma^+) + X_2 (D_{\infty h}, {}^1\Sigma_g^+) \qquad \Delta E(X{=}Cl) = +78.1 \text{ kcal/mol} \quad \Delta E(X{=}Br) = +\ 76.8 \text{ kcal/mol} \tag{12}$$

The van der Waals bound isomers for MX_3 (MX_2···X) possess even lower dissociation energies against loss of X. The weak thermodynamic stability of the neutral MX_3 is due to the autolocalization of the one unpaired electron on only one or two halogen atoms after an electron detachment from the closed shell MX_3^- anions (Table 8).

TABLE 6: Comparison of the Experimental VDE's to Calculated VDE's at Three Levels of Theory for $CaCl_3^-$ and $CaBr_3^-$

			VDE(theo), eV		
feature	VDE(exp), eV	molecular orbital	TD-B3LYP/ 6-311+G(2df)	OVGF/ 6-311+G(2df)	ΔCCSD(T)/ 6-311+G(2df)
			$CaCl_3^-$ (D_{3h}, $^1A_1'$)		
X	6.62	$1a_2'$	5.72	6.68 (0.909)[a]	6.51
A	6.95	$1e''$	5.95	6.94 (0.911)[a]	
B	~7.0	$1a_2''$	5.95	6.97 (0.912)[a]	
C	7.11	$3e'$	6.29	7.00 (0.911)[a]	
D	7.20	$2e'$	6.52	7.24 (0.908)[a]	
E	~7.8	$1a_1'$	6.74	7.74 (0.909)[a]	
			$CaBr_3^-$ (D_{3h}, $^1A_1'$)		
X	6.10	$1a_2'$	5.35	6.23 (0.911)[a]	6.11
A	~6.4	$1e''$	5.56	6.50 (0.912)[a]	
B	~6.5	$1a_2''$	5.58	6.55 (0.913)[a]	
C	6.90	$3e'$	5.97	6.57 (0.912)[a]	
D	7.06	$2e'$	6.11	6.85 (0.909)[a]	
E	7.49	$1a_1'$	6.44	7.40 (0.910)[a]	

[a] Values in parentheses represent the pole strength of the OVGF calculation.

TABLE 7: Calculated VDE's for $BeCl_3^-$ and $BeBr_3^-$ at Three Levels of Theory

molecular orbital	TD-B3LYP/ 6-311+G(2df)	OVGF/ 6-311+G(2df)	ΔCCSD(T)/ 6-311+G(2df)
	$BeCl_3^-$ (D_{3h}, $^1A_1'$)		
$1a_2'$	5.46	6.15 (0.906)[a]	6.01
$1e''$	5.94	6.70 (0.907)[a]	6.57
$3e'$	6.40	6.72 (0.906)[a]	6.58
$1a_2''$	6.67	7.57 (0.909)[a]	
$2e'$	7.70	8.35 (0.903)[a]	
$2a_1'$	8.51	9.50 (0.902)[a]	
	$BeBr_3^-$ (D_{3h}, $^1A_1'$)		
$1a_2'$	5.03	5.65 (0.908)[a]	5.55
$1e''$	5.47	6.17 (0.909)[a]	6.06
$3e'$	5.89	6.16 (0.908)[a]	6.06
$1a_2''$	6.15	6.98 (0.909)[a]	
$2e'$	7.15	7.72 (0.903)[a]	
$2a_1'$	8.14	9.06 (0.899)[a]	

[a] Values in parentheses represent the pole strength of the OVGF calculation.

TABLE 8: Theoretical Adiabatic Detachment Energies (eV) for MX_3^- (M = Be, Mg. Ca; X = Cl, Br) at Four Levels of Theory

species	B3LYP/ 6-311+G*	MP2/ 6-311+G*	CCSD(T)/ 6-311+G*	CCSD(T)/ 6-311+G(2df)
$BeCl_3^-$	5.38	5.38	5.26	5.48
$BeBr_3^-$	4.95	4.94	4.88	5.05
$MgCl_3^-$	5.52	5.53	5.42	5.61
$MgBr_3^-$	5.12	5.14	5.05	5.22
$CaCl_3^-$	5.47	5.47	5.37	5.42
$CaBr_3^-$	5.12	5.11	5.05	5.10

Conclusions

We report a combined experimental and theoretical investigation of the alkaline earth superhalogen species MX_3^- (M = Be, Mg, Ca; X = Cl, Br). Photoelectron spectra were obtained for MX_3^- (M= Mg, Ca; X = Cl, Br) and confirmed their high electron binding energies. The measured electron binding energies for all the MX_3^- species are much higher than the electron binding energies of the corresponding X^- halogens, suggesting the MX_3^- anions are truly superhalogens. Theoretical calculations were performed for all the MX_3^- species, and the theoretical VDE's for them were used to interpret the photoelectron spectra. Good agreement was obtained between the experimental and theoretical data.

The ground-state photodetachment feature for each MX_3^- anion is broad, indicating a large geometry change between the anion and neutral ground state. All the MX_3^- anions were found to possess a closed shell D_{3h} structure, whereas the neutral MX_3 species were found to possess an open shell C_{2v} structure. The ground-state structure for all MX_3 neutrals can be described as $(X_2^-)M^{2+}X^-$, and a XMX···X van der Waals complex was found to be a higher lying isomer. The large geometry change between the MX_3^- anions and the MX_3 neutral is reflected in the much lower calculated ADE values for these species relative to their corresponding VDE's. In fact, the ADE's were not detected experimentally because the Franck−Condon factors for the transition to the ground vibrational levels were negligible. Nevertheless, the computed ADE's for all the MX_3^- anions are much higher than that of Cl^-, and these species are true "superhalogens."

Acknowledgment. The theoretical work done at Utah State University was supported by the donors of the Petroleum Research Fund (ACS-PRF# 38242-AC6) administered by the American Chemical Society and by National Science Foundation (CHE-0404937). The experimental work done at Washington State was supported by the National Science Foundation (CHE-0349426) and performed at the W. R. Wiley Environmental Molecular Sciences Laboratory, a national scientific user facility sponsored by DOE's Office of Biological and Environmental Research and located at Pacific Northwest National Laboratory, which is operated for DOE by Battelle.

Supporting Information Available: Calculated molecular properties of Cl_2, Cl_2^-, Br_2, Br_2^-, $BeCl^-$, BeCl, $BeBr^-$, BeBr, $MgCl^-$, MgCl, $MgBr^-$, MgBr, $CaCl^-$, CaCl, $CaBr^-$, CaBr, $BeCl_2$, $BeBr_2$, $MgCl_2$, $MgBr_2$, $CaCl_2$, and $CaBr_2$. This material is available free of charge via the Internet at http://pubs.acs.org.

References and Notes

(1) Hotop, H.; Lineberger, W. C. *J. Phys. Chem. Ref. Data* **1985**, *14*, 731.
(2) Gutsev, G. L.; Boldyrev, A. I. *Chem. Phys.* **1981**, *56*, 277.
(3) Gutsev, G. L.; Boldyrev, A. I. *Zh. Neorg. Khim.* **1981**, *26*, 2353, 2357.
(4) Gutsev, G. L.; Boldyrev, A. I. *Adv. Chem. Phys.* **1985**, *61*, 169.
(5) Hay, P. J.; Wadt, W. R.; Kahn, L. R.; Raffenetti, R. C.; Phillips, D. H. *J. Chem. Phys.* **1979**, *71*, 1767.
(6) Bloor, J. E.; Sherrod, R. E. *J. Am. Chem. Soc.* **1980**, *102*, 4333.
(7) Gutsev, G. L.; Boldyrev, A. I. *Chem. Phys. Lett.* **1981**, *84*, 352.
(8) Gutsev, G. L.; Boldyrev, A. I. *Chem. Phys. Lett.* **1983**, *101*, 441.
(9) Gutsev, G. L.; Boldyrev, A. I. *Chem. Phys.* **1984**, *108*, 250.
(10) Gutsev, G. L.; Boldyrev, A. I. *Chem. Phys.* **1984**, *108*, 254.
(11) Gutsev, G. L.; Boldyrev, A. I. *Mol. Phys.* **1984**, *53*, 23.
(12) Sakai, Y.; Miyoshi, E. *J. Chem. Phys.* **1987**, *87*, 2885.
(13) Miyoshi, E.; Sakai, Y.; Murakami, A.; Iwaki, H.; Terashima, H.; Shoda, T.; Kawaguchi, T. *J. Chem. Phys.* **1988**, *89*, 4193.
(14) Mota, F.; Novoa, J. J.; Ramirez, A. C. *J. Mol. Struct.: THEOCHEM* **1988**, *43*, 153.
(15) Zakzhevskii, V. G.; Boldyrev, A. I. *J. Chem. Phys.* **1990**, *93*, 657.
(16) Komel, C.; Palm, G.; Ahlrichs, R.; Bar, M.; Boldyrev, A. I. *Chem. Phys. Lett.* **1990**, *173*, 151.
(17) Boldyrev, A. I.; von Niessen, W. *Chem. Phys.* **1991**, *155*, 71.
(18) Weikert, H.-G.; Cederbaum, L. S.; Tarantelli, F.; Boldyrev, A. I. *Z. Phys. D* **1991**, *18*, 299.
(19) Gutsev, G. L. *Chem. Phys. Lett.* **1991**, *184*, 305.
(20) Scheller, M. K.; Cederbaum, L. S. *J. Phys. B* **1992**, *25*, 2257.
(21) Boldyrev, A. I.; Simons, J. *J. Chem. Phys.* **1992**, *97*, 2826.
(22) Scheller, M. K.; Cederbaum, L. S. *J. Chem. Phys.* **1993**, *99*, 441.
(23) Ortiz, J. V. *J. Chem. Phys.* **1993**, *99*, 6727.
(24) Ortiz, J. V. *Chem. Phys. Lett.* **1993**, *214*, 467.
(25) Weikert, H.-G.; Cederbaum, L. S. *J. Chem. Phys.* **1993**, *99*, 8877.
(26) Gutsev, G. L. *J. Chem. Phys.* **1993**, *98*, 444.
(27) Gutsev, G. L. *J. Chem. Phys.* **1993**, *99*, 3906.
(28) Scheller, M. K.; Cederbaum, L. S. *J. Chem. Phys.* **1994**, *100*, 8934.
(29) Gutsev, G. L.; Les, A.; Adamowicz, L. *J. Chem. Phys.* **1994**, *100*, 8925.

(30) Weikert, H.-G.; Meyer, H.-D.; Cederbaum, L. S. *J. Chem. Phys.* **1996**, *104*, 7122.

(31) Gutowski, M.; Boldyrev, A. I.; Simons, J.; Raz, J.; Blazejowski, J. *J. Am. Chem. Soc.* **1996**, *118*, 1173.

(32) Gutsev, G. L.; Bartlett, R. J.; Boldyrev, A. I.; Simons, J. *J. Chem. Phys.* **1997**, *107*, 3867.

(33) Gutsev, G. L.; Jena, P.; Bartlett, R. J. *Chem. Phys. Lett.* **1998**, *292*, 289.

(34) Sobczyk, M.; Sawicka, A.; Skurski, P. *Eur. J. Inorg. Chem.* **2003**, *2003*, 3790.

(35) Bartlett, N. *Angew. Chem., Int. Ed. Engl.* **1968**, *7*, 433.

(36) Jensen, D. E. *Trans. Faraday Soc.* **1969**, *65*, 2123.

(37) Jensen, D. E.; Miller, W. J. *J. Chem. Phys.* **1970**, *53*, 3287.

(38) Ferguson, E. E.; Dunkin, D. B.; Feshenfeld, F. C. *J. Chem. Phys.* **1972**, *57*, 1459.

(39) Miller, W. J. *J. Chem. Phys.* **1972**, *57*, 2354.

(40) Burgess, J.; Haigh, I. H.; Peacock, R. D.; Taylor, P. *J. Chem. Soc., Dalton Trans.* **1974**, *10*, 1064.

(41) Leffert, C. B.; Tang, S. Y.; Rothe, E. W.; Cheng, T. C. *J. Chem. Phys.* **1974**, *61*, 4929.

(42) Cooper, C. D.; Compton, R. N. *Bull. Am. Phys. Soc.* **1974**, *19*, 1067.

(43) Tang, S. Y.; Reck, G. P.; Rothe, E. W. *Bull. Am. Phys. Soc.* **1974**, *19*, 1173.

(44) Boring, M.; Wood, J. H.; Moskowtiz, J. W. *J. Chem. Phys.* **1974**, *61*, 3800.

(45) Gould, R. K.; Miller, W. J. *J. Chem. Phys.* **1975**, *62*, 644.

(46) Beauchamp, J. L. *J. Chem. Phys.* **1976**, *64*, 929.

(47) Mathur, B. P.; Rothe, E. W.; Tang, S. Y.; Mahajan, K. *J. Chem. Phys.* **1976**, *64*, 1247.

(48) Compton, R. N. *J. Chem. Phys.* **1977**, *66*, 4478.

(49) Mathur, B. P.; Rothe, E. W.; Reck, G. P. *J. Chem. Phys.* **1977**, *67*, 377.

(50) Compton, R. N.; Reinhart, P. W.; Cooper, C. D. *J. Chem. Phys.* **1978**, *68*, 2023.

(51) Pyatenko, A. T.; Gorokhov, L. N. *Chem. Phys. Lett.* **1984**, *105*, 205.

(52) Compton, R. N. In *Photophysics and Photochemistry in the Vacuum Ultraviolet*; McGlynn, S. P., Findley, C. L., Huebner, R. A., Eds.; NATO ASI Series C: Mathematical and Physical Sciences; Reidel: Boston, MA, 1985; Vol. 142, p 261.

(53) Igolkina, N. A.; Nikitin, M. I.; Boltalina, O. V.; Sidorov, L. V. *High Temp. Sci.* **1986**, *21*, 111.

(54) Igolkina, N. A.; Nikitin, M. I.; Sidorov, L. V.; Boltalina, O. V. *High Temp. Sci.* **1987**, *23*, 89.

(55) Borshchevskii, A. Ya.; Boltalina, O. V.; Sorokin, I. D.; Sidorov, L. N. *J. Chem. Thermodyn.* **1988**, *20*, 523.

(56) Sidorov, L. N.; Boltalina, O. V.; Borshchevski, A. Ya. *Int. J. Mass Spectrom. Ion Processes* **1989**, *87*, R1.

(57) Boltalina, O. V.; Borshchevskii, A. Ya.; Sidorov, L. V. *Russ. J. Phys. Chem.* **1991**, *65*, 466.

(58) Scheller, M. K.; Compton, R. N.; Cederbaum, L. S. *Science* **1995**, *270*, 1160.

(59) Wang, X.-B.; Ding, C.-F.; Wang, L.-S.; Boldyrev, A. I.; Simons, J. *J. Chem. Phys.* **1999**, *110*, 4763.

(60) Ashman, C.; Khanna, S. N.; Pederson, M. R.; Kortus, J. *Phy. Rev. B* **2000**, *62*, 16956.

(61) Rao, B. K.; Jena, P.; Burkart, S.; Ganteför, G.; Seifert, G. *Phys. Rev. Lett.* **2001**, *86*, 692.

(62) Pradhan, P.; Ray, A. K. *THEOCHEM* **2005**, *716*, 109.

(63) Xu, W.; Li, G.; Yu, G.; Zhao, Y.; Li, Q.; Xie, Y.; Schaefer, H. F., III. *J. Phys. Chem. A* **2003**, *107*, 258.

(64) Alexandrova, A. N.; Boldyrev, A. I.; Fu, Y. J.; Yang, X.; Wang, X.-B.; Wang, L. S. *J. Chem. Phys.* **2004**, *121*, 5709.

(65) Anusiewicz, I.; Skurski, P. *Chem. Phys. Lett.* **2002**, *358*, 426.

(66) Anusiewicz, I.; Sobczyk, M.; Dabkowska, I.; Skurski, P. *Chem. Phys.* **2003**, *291*, 171.

(67) Wang, L. S.; Ding, C. F.; Wang, X. B.; Barlow, S. E. *Rev. Sci. Instrum.* **1999**, *70*, 1957.

(68) Becke, A. D. *J. Chem. Phys.* **1993**, *98*, 5648.

(69) Vosko, S. H.; Wilk, L.; Nusair, M. *Can. J. Phys.* **1980**, *58*, 1200.

(70) Lee, C.; Yang, W.; Parr, R. G. *Phys. Rev. B* **1988**, *37*, 785.

(71) Miehlich, B.; Savin, A.; Stoll, H.; Preuss, H. *Chem. Phys. Lett.* **1989**, *157*, 200.

(72) Krishnan, R.; Binkley, J. S.; Seeger, R.; Pople, J. A. *J. Chem. Phys.* **1980**, *72*, 650.

(73) Blaudeau, J.-P.; McGrath, M. P.; Curtiss, L. A.; Radom, L. *J. Chem. Phys.* **1997**, *107*, 5016.

(74) Binning, R. C., Jr.; Curtiss, L. A. *J. Comput. Chem.* **1990**, *11*, 1206.

(75) Curtiss, L. A.; McGrath, M. P.; Blaudeau, J.-P.; Davis, N. E.; Binning, R. C., Jr.; Radom, L. *J. Chem. Phys.* **1995**, *103*, 6104.

(76) McGrath, M. P.; Radom, L. *J. Chem. Phys.* **1991**, *94*, 511.

(77) Clark, T.; Chandrasekhar, J.; Spitznagel, G. W.; Schleyer, P. v. R. *J. Comput. Chem.* **1983**, *4*, 294.

(78) Frisch, M. J.; Pople, J. A.; Binkley, J. S. *J. Chem. Phys.* **1984**, *80*, 3265.

(79) Head-Gordon, M.; Pople, J. A.; Frisch, M. J. *Chem. Phys. Lett.* **1988**, *153*, 503.

(80) Frisch, M. J.; Head-Gordon, M.; Pople, J. A. *Chem. Phys. Lett.* **1990**, *166*, 275.

(81) Frisch, M. J.; Head-Gordon, M.; Pople, J. A. *Chem. Phys. Lett.* **1990**, *166*, 281.

(82) Head-Gordon, M.; Head-Gordon, T. *Chem. Phys. Lett.* **1994**, *220*, 122.

(83) Saebo, S.; Almof, J. *Chem. Phys. Lett.* **1989**, *154*, 83.

(84) Cizek, J. *Adv. Chem. Phys.* **1969**, *14*, 35.

(85) Purvis, G. D.; Bartlett, R. J. *J. Chem. Phys.* **1982**, *76*, 1910.

(86) Scuseria, G. E.; Janssen, C. L.; Schaefer, H. F., III. *J. Chem. Phys.* **1988**, *89*, 7382.

(87) Scuseria, G. E.; Schaefer, H. F., III. *J. Chem. Phys.* **1989**, *90*, 3700.

(88) Head-Gordon, M.; Pople, J. A.; Raghavachari, K. *J. Chem. Phys.* **1987**, *87*, 5968.

(89) Cederbaum, L. S. *J. Phys. B* **1975**, *8*, 290.

(90) Niessen, W. von; Shirmer, J.; Cederbaum, L. S. *Comput. Phys. Rep.* **1984**, *1*, 57.

(91) Zakrzewski, V. G.; Ortiz, J. V. *Int. J. Quantum Chem., Quantum Chem. Symp.* **1994**, *28*, 23.

(92) Zakrzewski, V. G.; Ortiz, J. V. *Int. J. Quantum Chem.* **1995**, *53*, 583.

(93) (a) Zakrzewski, V. G.; Ortiz, J. V.; Nichols, J. A.; Heryadi, D.; Yeager, D. L.; Golab, J. T. *Int. J. Quantum Chem.* **1996**, *60*, 29. (b) Ortiz, J. V. *Adv. Quantum Chem.* **1999**, *35*, 33.

(94) Stratmann, R. E.; Scuseria, G. E.; Frisch, M. J. *J. Chem. Phys.* **1998**, *109*, 8218.

(95) Bauernschmitt, R.; Ahlrichs, R. *Chem. Phys. Lett.* **1996**, *256*, 454.

(96) Casida, M. E.; Jamorski, C.; Casida, K. C.; Salahub, D. R. *J. Chem. Phys.* **1998**, *108*, 4439.

(97) Becke, A. D. *Phys. Rev. A* **1988**, *38*, 3098.

(98) Burke, K.; Perdew, J. P.; Wang, Y. In *Electronic Density Functional Theory: Recent Progress and New Directions*; Dobson, J. F., Vignale, G., Das, M. P., Eds.; Plenum: 1998.

(99) Perdew, J. P. In *Electronic Structure of Solids '91*; Ziesche, P., Eschrig, H., Eds.; Akademie Verlag: Berlin, Germany, 1991; Vol. 11.

(100) Perdew, J. P.; Chevary, J. S.; Vosko, S. H.; Jackson, K. A.; Pederson, M. R.; Singh, D. J.; Fiolhais, C. *Phys. Rev. B* **1992**, *46*, 6671.

(101) Perdew, J. P.; Chevary, J. S.; Vosko, S. H.; Jackson, K. A.; Pederson, M. R.; Singh, D. J.; Fiolhais, C. *Phys. Rev. B* **1993**, *48*, 4978.

(102) Perdew, J. P.; Burke, K.; Wang, Y. *Phys. Rev. B* **1996**, *54*, 16533.

(103) Frisch, M. J.; Trucks, G. M.; Schlegel, H. B.; Scuseria, G. E.; Robb, M. A.; Cheeseman, J. R.; Montgomery, J. A., Jr.; Vreven, T.; Kudin, K. N.; Burant, J. C.; Millam, J. M.; Iyengar, S. S.; Tomasi, J.; Barone, V.; Mennucci, B.; Cossi, M.; Scalmani, G.; Rega, N.; Petersson, G. A.; Nakatsuji, H.; Hada, M.; Ehara, M.; Toyota, K.; Fakuda, R.; Hasegawa, J.; Ishida, M.; Nakajima, T.; Honda, Y.; Kitao, O.; Nakai, H.; Klene, M.; Li, X.; Knox, J. E.; Hratchian, H. P.; Cross, J. B.; Adamo, C.; Jaramillo, J.; Gomperts, R.; Stratmann, R. E.; Yazyev, O.; Austin, A. J.; Cammi, R.; Pomelli, C.; Ochterski, J. W.; Ayala, P. Y.; Morokuma, K.; Voth, G. A.; Salvador, P.; Dannenberg, J. J.; Zakrzewski, V. G.; Dapprich, S.; Daniels, A. D.; Strain, M. C.; Farkas, O.; Malick, D. K.; Rabuck, A. D.; Raghavachari, K.; Foresman, J. B.; Ortiz, J. V.; Cui, Q.; Baboul, A. G.; Clifford, S.; Cioslowski, J.; Stefanov, B. B.; Liu, G.; Liashenko, A.; Piskorz, P.; Komaromi, I.; Martin, R. L.; Fox, D. J.; Keith, T.; Al-Laham, M. A.; Peng, C. Y.; Nanayakkara, A.; Challacombe, M.; Gill, P. M. W.; Johnson, B. G.; Chen, W.; Wong, M. W.; Gonzales, C.; Pople, J. A. *Gaussian 03*, revision A.1; Gaussian, Inc.: Pittsburgh, PA, 2003.

(104) Frisch, M. J.; Trucks, G. M.; Schlegel, H. B.; Scuseria, G. E.; Robb, M. A.; Cheeseman, J. R.; Zakrzewski, V. G.; Montgomery, J. A.; Stratmann, R. E.; Burant, J. C.; Dapprich, S.; Millam, J. M.; Daniels, A. D.; Kudin, K. N.; Strain, M. C.; Farkas, O.; Tomasi, J.; Barone, V.; Cossi, M.; Cammi, R.; Mennucci, B.; Pomelli, C.; Adamo, C.; Clifford, S.; Ochterski, J. W.; Petersson, G. A.; Ayala, P. Y.; Cui, Q.; Morokuma, K.; Malick, D. K.; Rabuck, A. D.; Raghavachari, K.; Foresman, J. B.; Cioslowski, J.; Ortiz, J. V.; Stefanov, B. B.; Liu, G.; Liashenko, A.; Piskorz, P.; Komaromi, I.; Gomperts, R.; Martin, R. L.; Fox, D. J.; Keith, T.; Al-Laham, M. A.; Peng, C. Y.; Nanayakkara, A.; Gonzales, C.; Challacombe, M.; Gill, P. M. W.; Johnson, B. G.; Chen, W.; Wong, M. W.; Andres, J. L.; Head-Gordon, M.; Replogle, E. S.; Pople, J. A. *Gaussian 98*, revision A.1; Gaussian, Inc.: Pittsburgh, PA, 1998.